Springer

KSME

Journal of Mechanical Science and Technology 29 (8) (2015) 3121~3129
www.springerlink.com/content/1738-494x(Print)/1976-3824(Online)
DOI 10.1007/s12206-015-0710-0

Fault diagnosis of rolling bearing based on second generation wavelet denoising and morphological filter †

Lingjie Meng[1,2], Jiawei Xiang[1,*], Yongteng Zhong[1] and Wenlei Song[1]

[1]*College of Mechanical and Electrical Engineering, Wenzhou University, Wenzhou, 325035, China*
[2]*School of Mechanical and Electrical Engineering, Guilin University of Electronic Technology, Guilin, 541004, China*

(Manuscript Received October 27, 2014; Revised February 24, 2015; Accepted March 14, 2015)

Abstract

Defective rolling bearing response is often characterized by the presence of periodic impulses. However, the in-situ sampled vibration signal is ordinarily mixed with ambient noises and easy to be interfered even submerged. The hybrid approach combining the second generation wavelet denoising with morphological filter is presented. The raw signal is purified using the second generation wavelet. The difference between the closing and opening operator is employed as the morphology filter to extract the periodicity impulsive features from the purified signal and the defect information is easily to be extracted from the corresponding frequency spectrum. The proposed approach is evaluated by simulations and vibration signals from defective bearings with inner race fault, outer race fault, rolling element fault and compound faults, respectively. Results show that the ambient noises can be fully restrained and the defect information of the above defective bearings is well extracted, which demonstrates that the approach is feasible and effective for the fault detection of rolling bearing.

Keywords: Second generation wavelet transform; Denoising; Morphological filter; Rolling bearing; Fault diagnosis

1. Introduction

The rotating machinery has been widely used in almost all of the industry sections. Therefore, it is extremely significant to detect the fault of rotating machinery [1-3]. For as the rolling bearing being the most widely used standardized parts in rotating machinery, the mechanical fault diagnosis are always carried out regarding it [4-6]. When a fault exists in one surface of a bearing, the vibration signal is characterized by the presence of periodic impulses. How to extract the interesting information which represents the bearing fault feature from the periodicity impacts is the crux for condition monitoring and fault diagnosis. However, the vibration signals are ordinarily non-stationary and represent non-linear processes [7], their frequency components will change with time [8]. Therefore, the adaptive analysis methods such as the wavelet transform (WT) [9], ensemble empirical mode decomposition (EEMD) [10] and local mean decomposition (LMD) [11, 12], etc., have been the good choices to deal with the non-stationary signals. However, those methods also still suffer from the following disadvantages, e.g., the WT method has been widely applied for its upstanding time-frequency localization peculiarity, but the appropriate choices of the wavelet base function or the certain frequency bands with fault information need to be solved. The EEMD method, which developed from the empirical mode decomposition (EMD) method [13-16], improves the major drawback of mode mixing of EMD method via defining the true intrinsic mode functions (IMFs) as the mean of an ensemble of trials, each consisting of the signal corrupted by additive white noise of finite variance. However, in order to offset the remaining noise sufficiently, an ensemble number of a few hundred might be required, that is obvious inefficient when dealing with large volumes of data. The LMD method, developed by Smith [17], ca decompose any complicated signals into a set of product functions (PFs) which have been proved to be having more reasonable and meaningful interpretations than the IMFs [18]. However, the decomposition results of LMD method are easy to be interfered by noises, and the deficiency of low computational efficiency still exists as that case of EEMD.

In recent years, a novel morphological signal processing method has been applied to detect faults in rotating machinery for its adaptive performance in extracting the shape information in addition to its simple and rapid calculation [19, 20]. In 2003, Nikolaou and Antoniadis firstly introduced the method to detect faults of rolling bearing and the results showed this method was more efficient for low noise signals than for high

*Corresponding author. Tel.: +86 15167425460, Fax.: +86 577 86689138
E-mail address: wxw8627@163.com
† Recommended by Associate Editor Cheolung Cheong

noise signals [21]. Due to the in-situ sampled vibration signal is ordinarily mixed with ambient noises, it is necessary to carry on denoising pretreatment to the raw signal before applying the morphological method. Unlike the traditional WT, the second generation wavelet (SGW) [22] is a flexible wavelet construction method which is independent of the Fourier transform. Applying SGW to the denoising pretreatment will provide a faster and a more effective algorithm than the traditional WT [23-27].

For the above reasons, we propose a hybrid approach based on SGW denoising and morphological filter to purify the raw signal and to extract the defect information, respectively. The outline of this paper is as follows. The fundamental theories of second generation wavelet denoising and morphological filter are briefly summarized in Sec. 2. In Sec. 3, the hybrid approach is presented and further validated by simulation analysis. Sec. 4 demonstrates the experimental results using the proposed approach to extract the fault features from vibration signals of the defective bearings with inner race fault, outer race fault, rolling element fault and compound faults, respectively. Finally, conclusion remarks are drawn in Sec. 5.

2. Methods

2.1 Denoising algorithm based on SGW

SGW is a new wavelet construction method using lifting scheme in the time domain [22]. The main feature of the SGW is that it provides an entirely spatial domain interpretation of the transform to replace the traditional frequency domain based constructions. The decomposition stage of SGW can be summarized as follows.

Consider a signal $X = \{x_k, k \in Z\}, k = 1,2,\cdots,L$ .The approximation signal $\{s_{j+1}(k)\}$ of X on level $j+1$ is split into even indexed samples $\{s_j(2k)\}$ and odd indexed samples $\{s_j(2k+1)\}$ on level j . Predicting an odd indexed sample with N neighbors of the even indexed samples on level j , the detail signal $d_j(k)$ is obtained as:

$$d_j(k) = s_{j+1}(2k+1) - \sum_{m=1}^{N} p(m) s_{j+1}(2m+k-N) \tag{1}$$

where $p(m)$ is a prediction coefficient, $m = 1, 2,\cdots, N$. $P = \left[p(1),\cdots,p(N)\right]^T$ represents a predictor for detail signal calculation.

Then M number of detail signals $d_j(k)$ obtained from Eq. (1) are adopted to update the even indexed samples $\{s_j(2k)\}$, the approximation signal $s_j(k)$ is

$$s_j(k) = s_{j+1}(2k) - \sum_{m=1}^{M} u(m) d_j(m+k-M/2-1) \tag{2}$$

where $u(m)$ is an update coefficient, $m = 1,2,\cdots,M$. $U = \left[u(1),\cdots,u(M)\right]^T$ represents an updater for approximation signal calculation.

The reconstruction stage of SGW is a reverse procedure of the decomposition stage. The operators P and U are built by means of Interpolating subdivision method (ISM) [28]. In the process of data collection, the length of data is set to the integer power of two, and being different from the orthogonal wavelet transform, the SGW is the biorthogonal wavelet transform, therefore, the value of N or M is ordinarily being the even during the decomposition stage of SGW, and choosing different N and M, scaling function and wavelet function with different vanishing moment number can be available [29]. Perform multi-scale decompositions for the raw signal, and then process the detail signal at each level using threshold processing, the purified signal is obtained by reconstructing the approximation signal and the denoised detail signals. According to Ref. [30], by imposing $N = 4$, $M = 4$ and three levels decompositions are proper for vibration signal denoising of rolling bearing.

In the threshold processing, the most popular denoising methods include the soft-threshold method and the hard-threshold method. Donoho [31] gave the threshold $\tau = \sigma\sqrt{2\log N}$. Where σ is the standard deviation of detail signal's noise estimation at each level, N is the length of signal. We can see that Donoho's threshold is varying with N, and when N is too large, the threshold may over smooth the signal. To solve this problem, Pan proposed a more intuitive threshold scheme, $\tau_l = c \bullet \sigma$, where c is a constant [32]. According to his research [33], by imposing c between 3 and 4 and the hard-threshold method will achieve better denoising effect.

2.2 Morphological filter

Morphological method was initially introduced in image processing by Serra [34], and later on, it was used in other areas such as signal processing [35]. The basic concept of morphological signal processing is to modify the shape of a signal, by transforming it through its intersection with another object called the structuring elements (SEs). There are four basic morphological operations, namely dilation, erosion, closing and opening, which form the foundation of morphological method.

Let $f(n)$ be the original one dimensional (1D) discrete signal, which is the function over a domain $F = (0,1,\cdots,N-1)$, and $g(m)$ be the SEs, which is the discrete function over a domain $G = (0,1,\cdots,M-1)(M \le N)$. The above four basic operations can be defined as follows:

Dilation:

$$(f \oplus g)(n) = \max\{f(n-m) + g(m)\}$$
$$\{1 \le n \le N; 1 \le m \le M\}. \tag{3}$$

Erosion:

$$(f \Theta g)(n) = \min\{f(n+m) - g(m)\} \ \{1 \le n \le N; 1 \le m \le M\} \tag{4}$$

Table 1. Properties of the morphological operators to impulsive features.

Morphological operators	Positive impulse	Negative impulse
Dilation	Smoothing	Reducing
Erosion	Reducing	Smoothing
Closing	Preserving	Reducing
Opening	Reducing	Preserving

$$\text{Closing}: \ (f \bullet g)(n) = (f \oplus g \Theta g)(n) \quad (5)$$

$$\text{Opening}: \ (f \circ g)(n) = (f \Theta g \oplus g)(n) \quad (6)$$

where $\oplus$, Θ , $\bullet$ and $\circ$ denote the operators for dilation, erosion, closing and opening operations, respectively. The properties of the operations to impulsive features are shown in Table 1, the closing and opening operator can be applied to detect positive and negative impulses, respectively.

In Nikolaou's study [21], closing operator was adopted to extract impulsive components from the raw signal and only positive impulses were detected. However, there are sharp peaks with both positive and negative amplitude in vibration response of defective rolling element bearing, although closing operation indeed extracts some useful information from the signal, but loses the geometric characteristics of the signal which may help to fault diagnosis. In order to detect bi-directional impulsive components, according to the properties of the operators, the difference (DIF) filter is used in this paper as follows:

$$\begin{aligned} DIF(f(n)) &= (f \bullet g)(n) - (f \circ g)(n) \\ &= (f \bullet g)(n) - f(n) + f(n) - (f \circ g)(n). \end{aligned} \quad (7)$$

In Eq. (7), $(f \bullet g)(n) - f(n)$ and $f(n) + (f \circ g)(n)$ are two types of the morphological Top-hat transform [36], $(f \bullet g)(n) - f(n)$ is called the black Top-Hat transform, which is used to extract negative impulsive features. $f(n) + (f \circ g)(n)$ is called the white Top-Hat transform, which is used to extract positive impulsive features. Therefore, the DIF filter can be used to extract the positive and negative impulsive features simultaneously.

SEs is another sticking point except the morphological operators, the attributes of the SEs are controlled by its shape, height (Amplitude), and length (Domain). There are various kinds of SEs, such as flat SEs, triangular SEs and semicircular SEs, etc. In the present, the flat SEs is employed because it appears to be quite appropriate for detecting impulses [37-39]. In order to retain the shape characters of the signal entirely, all the height of the flat SE is defined as zeros [39, 41]. All the studies show that the length of SEs is important for the morphological method [39-41], and the scholar developed various rules or guidelines for choosing the length of SEs. In theory, the shorter length of SEs, the more impulse features will be extracted when using the DIF filter. In order to obtain more impulse features of the vibration signal, the length of SEs is selected as several sampling points in the present investigation.

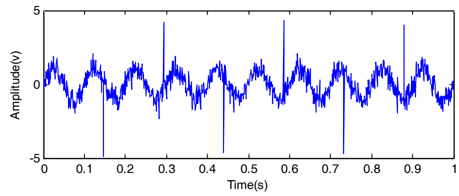

Fig. 1. The time domain waveform of the simulation signal $x(t)$.

3. The proposed fault diagnosis approach and its simulation analysis

Due to the SGW and morphological filter are all completely performed in time domain, and the two methods all have a fast computing algorithm, the combination of both can be applied to the real time monitor and signal processing, especially when dealing with large amounts of on-line vibration data. Based on these, the fault diagnosis approach based on SGW denoising and morphological filter is presented and described as follows.

(1) Collecting vibration signal of the defective bearings.

(2) Carrying on denoising pretreatment using the SGW denoising method. The length of the predictor and updater are all four and the purified signal will be decomposed into three levels in the present.

(3) Extracting the periodicity impulsive features using the morphological filter. The difference between the closing and opening operator is employed to extract the impulsive features.

(4) Applying the spectrum analysis on the impulsive components to extract the defect information.

To verify the effectiveness of the proposed approach, a synthesized signal is built to extract the impulsive features, suppress the harmonic features and the white noise feature. The simulation signal is defined as:

$$x(t) = x_1(t) + x_2(t) + x_3(t) \quad (8)$$

where $x_1(t) = \sin(20 \cdot \pi \cdot t)$ s a harmonic signal, $x_2(t)$ is the Gaussian noise (the ratio of the standard deviation of the Gaussian noise and that of $x_1(t)$ is 0.5), and $x_3(t)$ are a series of alternating positive and negative impulses (The repetition period and amplitude are 0.1465 s and 5, respectively). Suppose the sampling frequency is 1024 Hz and the length of sampling points is 1024, the time domain waveform of the simulation signal $x(t)$ is shown in Fig. 1. The harmonic wave and impulsive components are mixed with the Gaussian noise.

Applying the SGW denoising method to the simulation signal $x(t)$, the constant c of threshold scheme is 3.2. The purified signal is shown in Fig. 2. Compared with Fig. 1, the Gaussian noise is effectively removed; meanwhile, the impulsive features are well reserved.

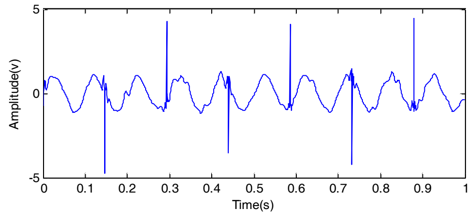

Fig. 2. The time domain waveform of the purified signal.

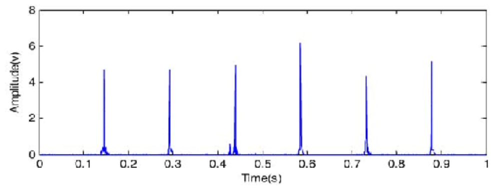

(a)

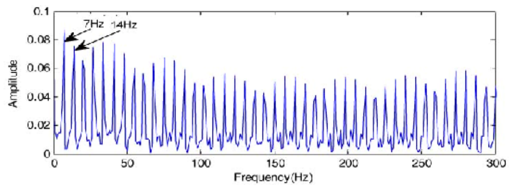

(b)

Fig. 3. The time domain waveform of the impulsive components and their frequency spectrums: (a) time domain waveform; (b) FFT spectrum.

After the denoising pretreatment, the DIF morphological filter is used to extract the impulsive features. Because the width of the added alternating positive or negative impulses is known in advance, therefore, the shorter SEs, a flat vector of null elements with length three, is employed to extract the impulsive features. The time domain waveform of the extracted impulsive components and their FFT spectrums are shown in Figs. 3(a) and (b), respectively. From Fig. 3(a), the alternating impulses are reserved; however, the harmonic signal $x_1(t)$ is ignored. It should be noted that the negative impulses are all changed into positive, but the phase information remains the same, and it has no influence on the results of fault diagnosis. The modulated frequency of the repetition periodic, $f = 1/0.1465 \approx 7Hz$, with its harmonics, e.g., 14 and 21 Hz,etc., are all clearly detected in Fig. 3(b).

By contrast, if applying the DIF morphological filter to the raw signal $x(t)$ directly without the SGW denoising pretreatment, the time domain waveform of the results and their FFT spectrums are shown in Figs. 4(a) and (b), respectively.

From Fig. 4(a), the impulse components are heavy mixed with the Gaussian noise. By comparing Fig. 4(b) with Fig. 3(b), the feature frequencies are confused by the noise and not as clear as that in Fig. 3(b). Overall, we can conclude that carrying on the denoising pretreatment before applying the DIF morphological filter is necessary, and the fault diagnosis approach based on SGW denoising and morphological filter is feasible and effective.

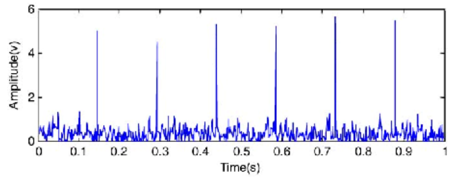

(a)

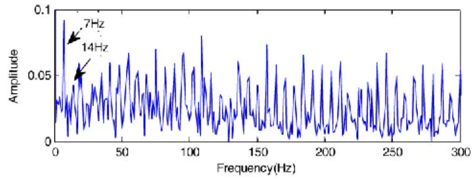

(b)

Fig. 4. The time domain waveform of the results and their frequency spectrums: (a) time domain waveform; (b) FFT spectrum.

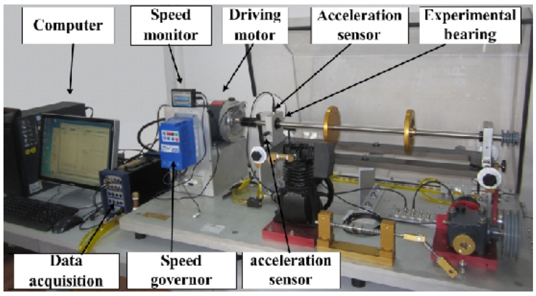

Fig. 5. The MFS-MG experimental platform.

4. Experimental investigations

In this section, the proposed approach is evaluated by defective bearings vibration signals. The vibration signals measured with the sample frequency of 25.6 kHz are performed on the MFS-MG experimental platform, as shown in Fig. 5.

During the experimental investigations, the defective bearing of the type ER-12K is installed on the left side of the shaft and the normal bearing is on the right side. The specifications of the bearing are listed as follows: the pitch diameter of the bearing is 33.4772 *mm*; the number of rolling element is 8; the rolling element diameter is 7.9375 *mm*; and the contact angle is 0º. A computer online monitoring system is available for data acquisition, and the vibration signals of bearings with four fault types (including inner race fault, outer race fault, rolling element fault and compound faults) were collected. Based on large numbers of experiments, the constant c of SGW denoising threshold scheme is 3.2, and in order to extract more impulse features, the flat SEs with length five is employed during the implementation process of the proposed approach.

4.1 Analysis of the defective bearing with an inner race fault

The defective bearing with an inner race fault is as shown in Fig. 6, and its typical vibration signal of at the rotating speed

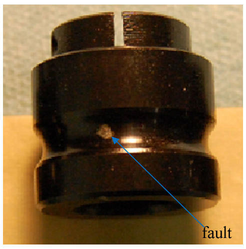

Fig. 6. The defective bearing with an inner race fault.

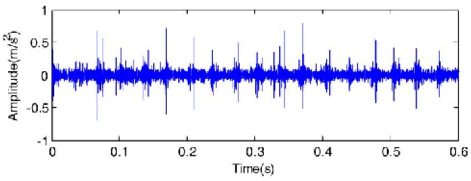

(a)

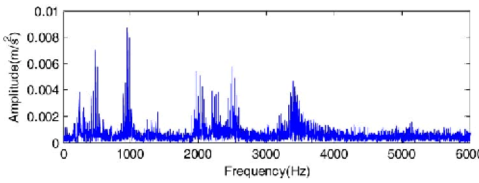

(b)

Fig. 7. The time domain waveform of bearing with an inner race fault and its frequency spectrum: (a) the time domain waveform; (b) the FFT spectrum.

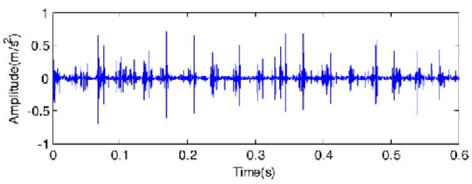

(a)

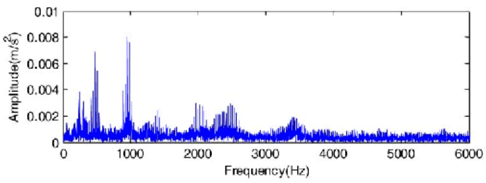

(b)

Fig. 8. The time domain waveform of the purified signal and its frequency spectrum: (a) the time domain waveform; (b) the FFT spectrum.

of 1792 rpm is shown in Fig. 7.

From Fig. 7, it can be seen that due to the defect present in the rolling bearing, the vibration signal presents the periodicity impacts features, but there exist very serious ambient noises. Applying the SGW denoising method to the vibration signal, the purified signal is shown in Fig. 8. By comparing Fig. 8 with Fig. 7, we get to know that the ambient noises are effectively suppressed. Meanwhile, the periodicity impacts features are well reserved.

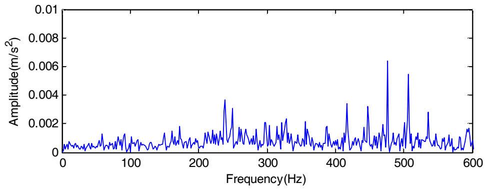

Fig. 9. The FFT spectrum on low frequency band of the purified signal.

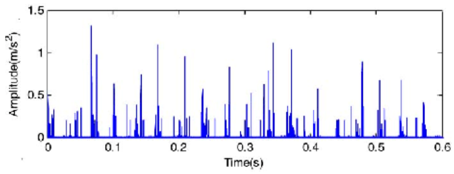

(a)

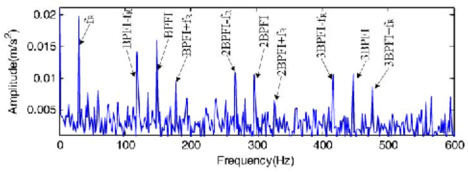

(b)

Fig. 10. The time domain waveform of resulting signal and its FFT spectrum: (a) the time domain waveform; (b) the FFT spectrum.

In general, the fault characteristic frequency components of rolling bearing always appear on low frequency band [42]. The FFT spectrum on low frequency band of the purified signal is shown in Fig. 9. Theoretically, the corresponding ball pass frequency in inner race (BPFI) is calculated as 147.85 Hz according to the specifications of the bearing. However, as shown in Fig. 9, the BPFI is not prominent and the existence of an inner race fault in the bearing is not confirmed.

Applying the DIF morphological filter to the purified signal, the time domain waveform of the resulting signal and its FFT spectrum are shown in Figs. 10(a) and (b), respectively. From Fig. 10(a), the impulsive features are effectively extracted. In the FFT spectrum, the inner defect frequency 147.85 Hz together with its second and third harmonics, 295.7 and 443.55 Hz, and side frequencies (147.85 ± 29.87 Hz, 295.7 ± 29.87 Hz, 443.55 ± 29.87 Hz) are prominent. The modulation frequency is 29.87 Hz (The frequency of rotor rotating, f_R). It reveals that the proposed approach is effective for the fault detection of rolling bearing.

4.2 Analysis of the defective bearing with an outer race fault

The defective bearing with an outer race fault is as shown in Fig. 11. Being the rotor of rotating speed of 1782 rpm, the raw signal of defective bearing with an outer race fault and the purified signal using the SGW denoising method are shown in Figs. 12(a) and (b), respectively. By comparison, it can be seen that the ambient noises are effectively suppressed.

The corresponding ball pass frequency in outer race (BPFO)

Fig. 11. The defective bearing with an outer race fault.

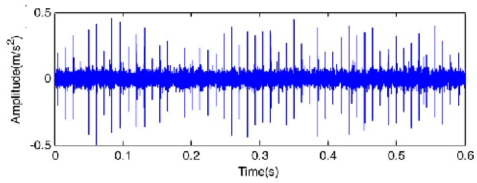

(a)

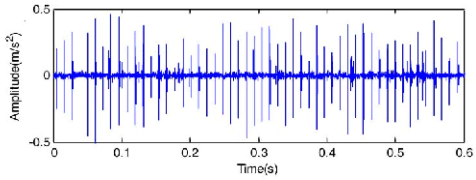

(b)

Fig. 12. The time domain waveform of the raw signal and the purified signal: (a) the original signal; (b) the purified signal.

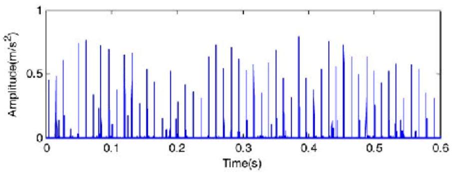

(a)

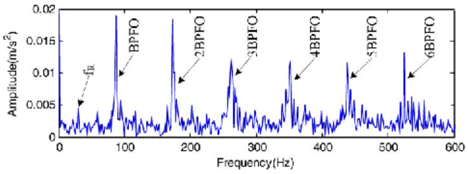

(b)

Fig. 13. The time domain waveform of resulting signal and its FFT spectrum: (a) the time domain waveform; (b) the FFT spectrum.

is 90.5 Hz . The frequency of rotor rotating f_R is 29.7 Hz . Applying the DIF morphological filter to the purified signal, the resulting signal is shown in Fig. 13, which shows that the BPFO together with its harmonics and the rotor rotating frequency f_R are all clearly detected. Therefore, we can conclude that there exists an outer race fault in the bearing.

4.3 Analysis of the defective bearing with a rolling element fault

The defective bearing with a rolling element fault is as shown in Fig. 14. Being the rotor of rotating speed of 1780,

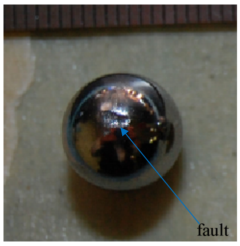

Fig. 14. The defective bearing with a rolling element fault.

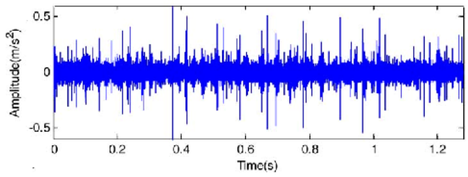

(a)

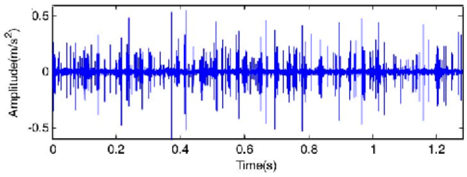

(b)

Fig. 15. The time domain waveform of the raw signal and the purified signal: (a) the original signal; (b) the purified signal.

the ball spin frequency (BSF) is 59.1 Hz , and the fundamental train frequency (FTF) is 11.21 Hz . The raw signal of defective bearing with a rolling element fault and the purified signal using the SGW denoising method are shown in Figs. 15(a) and (b), respectively. The comparison shows the effectiveness of the SGW denoising method.

Applying the DIF morphological filter to the purified signal, the time domain waveform of the resulting signal and its FFT spectrum are shown in Figs. 16(a) and (b), respectively. In the FFT spectrum, the BSF together with its harmonics, and the side frequencies modulated by the FTF are prominent. There is a good match between the expected spectrum features and the actual situation associated with the bearing with a rolling element fault.

4.4 Analysis of the defective bearing with the compound faults

When there exist the compound faults (including inner race fault, outer race fault and rolling element fault) in the bearing, the extraction of fault features gets even more complicated. A typical vibration signal of defective bearing with the compound faults at the rotor of rotating speed of 2389 rpm is shown in Fig. 17(a). Theoretically, the BPFI, BPFO and BSF are 197.1 Hz, 121.37 Hz and 79.32 Hz, respectively. The purified signal using the SGW denoising method is shown in Fig. 17(b) and the denoising effect is also obviously.

After applying the DIF morphological filter to the purified signal, the time domain waveform of the resulting signal and

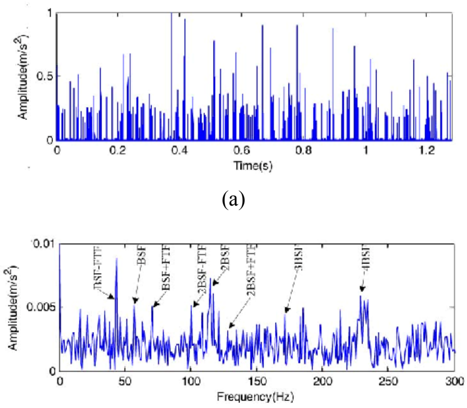

(a)

(b)

Fig. 16. The time domain waveform of resulting signal and its FFT spectrum: (a) the time domain waveform; (b) the FFT spectrum.

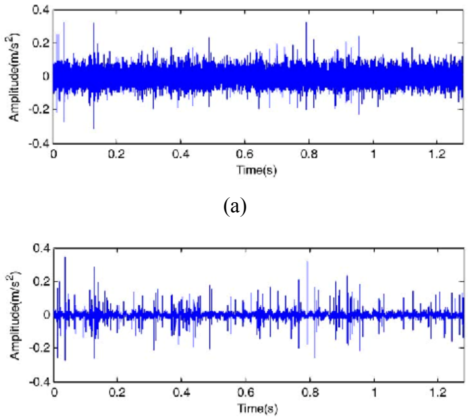

(a)

(b)

Fig. 17. The time domain waveform of the raw signal and the purified signal: (a) the original signal; (b) the purified signal.

its FFT spectrum are shown in Figs. 18(a) and (b), respectively. The fault characteristic frequency components including BPFI, BPFO and BSF are all prominent and found to be good matching with the corresponding feature frequencies.

It should be point that the performances of rolling element fault diagnosis and compound faults diagnosis are not excellent as that of inner race fault diagnosis or outer race fault diagnosis. Because when the rolling bearing operating at high speeds, the rolling elements are not only moving around the raceway, but also rotating on their own centre, then the defect point processed on the rolling element surface may not contact with the raceway. Therefore, for the case of rolling element fault diagnosis or compound faults diagnosis, the impulsive features present aperiodicity, even to be submerged, and difficult to be extracted. Because of this, the simple and effective fault diagnosis methods are urgently needed.

Through the above experimental investigations, it demonstrates that the proposed approach can effectively extract the fault features of defective bearings and obtains satisfactory results.

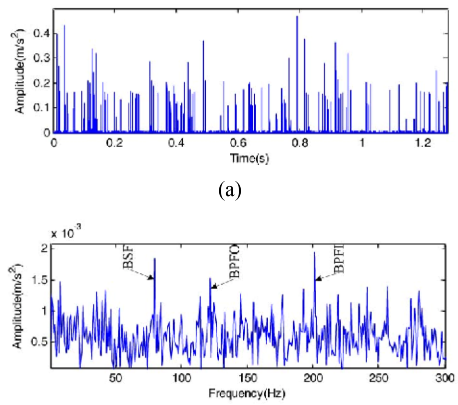

(a)

(b)

Fig. 18. The time domain waveform of resulting signal and its FFT spectrum: (a) the time domain waveform; (b) the FFT spectrum.

5. Conclusions

Aiming at the characterized response of the defective rolling bearing, the approach containing two parts, the denoising pretreatment and the fault feature extraction, is proposed in this paper. The SGW denoising is used to purify the raw signal, and the morphological filter is applied to extract the defect information. Its efficiency has been evaluated in simulation analysis and the experimental signals measured on the bearing with four kinds of fault. The results show that the present approach is feasible and effective to detect faults in rolling bearing. In addition, both of the two methods in the present approach have the advantages of simple formulation, rapid algorithm, and good performance, especially when dealing with large volumes of data. Therefore, it might be applied to real-time condition monitoring and fault diagnosis of rotary machinery.

Acknowledgments

The authors are grateful to the support from the National Science Foundation of China (No. 51175097) and the Zhejiang Provincial Natural Science Foundation for Excellent Young Scientists (No. LR13E050002), the Zhejiang Technologies R&D Program of China (No. 2014C31103) and the Zhejiang Qianjiang Talent Planning of China.

References

[1] B. S. Yang, T. Han and W. W. Hwang, Fault diagnosis of rotating machinery based on multi-class support vector machines, *Journal of Mechanical Science and Technology*, 19 (3) (2005) 846-859.

[2] M. Shi, D. Wang and J. Zhang, Nonlinear dynamic analysis of a vertical rotor-bearing system, *Journal of Mechanical Science and Technology*, 27 (1) (2013) 9-19.

[3] G. M. Lim, D. M. Bae and J. H. Kim, Fault diagnosis of rotating machine by thermography method on support vector

machine, *Journal of Mechanical Science and Technology*, 28 (8) (2014) 2947-2952.

[4] H. Li, Y. Zhang and H. Zheng, Bearing fault detection and diagnosis based on order tracking and Teager-Huang transform, *Journal of Mechanical Science and Technology*, 24 (3) (2010) 811-822.

[5] C. Li et al., Investigation on the stability of periodic motions of a flexible rotor-bearing system with two unbalanced disks, *Journal of Mechanical Science and Technology*, 28 (7) (2014) 2561-2579.

[6] Y. G. Luo et al., Stability of periodic motion on the rotor-bearing system with coupling faults of crack and rub-impact, *Journal of Mechanical Science and Technology*, 21 (6) (2007) 860-864.

[7] H. Ma et al., Time-frequency features of two types of coupled rub-impact faults in rotor systems, *Journal of Sound and Vibration*, 321 (2009) 1109-1128.

[8] F. Cong, J. Chen and G. Dong, Spectral kurtosis based on AR model for fault diagnosis and condition monitoring of rolling bearing, *Journal of Mechanical Science and Technology*, 26 (2) (2012) 301-306.

[9] Q. Hu et al., Fault diagnosis of rotating machinery based on improved wavelet package transform and SVMs ensemble, *Mechanical Systems and Signal Processing*, 21 (2) (2007) 688-705.

[10] Z. H. Wu and N. E. Huang, Ensemble empirical mode decomposition: a noise-assisted data analysis method, *Advances in Adaptive Data Analysis,* 1 (2009) 1-41.

[11] H. H. Liu and M. H. Han, A fault diagnosis method based on local mean decomposition and multi-scale entropy for roller bearings, *Mechanism and Machine Theory*, 75 (2014) 67-78.

[12] J. S. Cheng, K. Zhang and Y. Yang, An order tracking technique for the gear fault diagnosis using local mean decomposition method, *Mechanism and Machine Theory*, 55 (2012) 67-76.

[13] J. S. Cheng, D. J. Yu, J. S. Tang and Y. Yang, Local rub-impact fault diagnosis of the rotor systems based on EMD, *Mechanism and Machine Theory*, 44 (4) (2009) 784-791.

[14] H. Dong et al., Sifting process of EMD and its application in rolling element bearing fault diagnosis, *Journal of Mechanical Science and Technology*, 23 (8) (2009) 2000-2007.

[15] J. S. Cheng, D. J. Yu, J. S. Tang and Y. Yang, Application of SVM and SVD technique based on EMD to the fault diagnosis of the rotating machinery, *Shock and Vibration*, 16 (1) (2009) 89-98.

[16] Y. G. Lei et al., A review on empirical mode decomposition in fault diagnosis of rotating machinery, *Mechanical Systems and Signal Processing*, 35 (1) (2013) 108-126.

[17] J. S. Smith, The local mean decomposition and its application to EEG perception data, *Journal of the Royal Society Interface*, 2 (5) (2005) 443-454.

[18] Y. X. Wang, Z. J. He and Y. Y. Zi, A comparative study on the local mean decomposition and empirical mode decomposition and their applications to rotating machinery health diagnosis, *Journal of Vibration and Acoustics*, 132 (2) (2010) 021010.

[19] R. J. Hao, W. X. Lu and F. L. Chu, Mathematical morphology extracting method on roller bearing fault signals, *Proceedings of the CSEE*, 28 (26) (2008) 65-70.

[20] J. Wang et al., Application of improved morphological filter to the extraction of impulsive attenuation signals, *Mechanical Systems and Signal Processing*, 23 (1) (2009) 236-245.

[21] N. G. Nikolaou and I. A. Antoniadis, Application of morphological operators as envelope extractors for impulsive-type periodic signals, *Mechanical Systems and Signal Processing*, 17 (2003) 1147-1162.

[22] W. Sweldens, The lifting scheme: A construction of second generation wavelets, *SIAM Journal on Mathematical Analysis*, 29 (2) (1997) 511-546.

[23] H. K. Jiang et al., Gearbox fault diagnosis using adaptive redundant lifting scheme, *Mechanical Systems and Signal Processing,* 20 (8) (2006) 1992-2006.

[24] Z. Li et al., Customized wavelet denoising using intra-and inter-scale dependency for bearing fault detection, *Journal of Sound and Vibration*, 313 (1) (2008) 342-359.

[25] Z. Li et al., Bearing condition monitoring based on shock pulse method and improved redundant lifting scheme, *Mathematics and Computers in Simulation*, 79 (3) (2008) 318-338.

[26] Z. Li et al., Rotating machinery fault diagnosis using signal-adapted lifting scheme, *Mechanical Systems and Signal Processing*, 22 (3) (2008) 542-556.

[27] L. Ebadi et al., A review of applying second-generation wavelets for noise removal from remote sensing data, *Environmental Earth Sciences*, 70 (6) (2013) 2679-2690.

[28] R. L. Claypoole, G. M. Davis, W. Sweldens and R. Baraniuk, Nonlinear wavelet transforms for image coding via lifting, *IEEE Transactions on Image Process*, 12 (12) (2003) 1449-1459.

[29] R. L. Claypoole, R. G. Baraniuk and R. D. Nowak, Adaptive wavelet transforms via lifting, *Transactions of the International Conference on Acoustics, Speech and Signal Processing*, Seattle, WA (1998) 1513-1516.

[30] C. D. Duan, Z. J. He and H. K. Jiang, A sliding window feature extraction method for rotating machinery based on the lifting scheme, *Journal of Sound and Vibration*, 299 (4) (2007) 774-785.

[31] D. L. Donoho and J. M. Johnstone, Ideal spatial adaptation by wavelet shrinkage, *Biometrika*, 81 (3) (1994) 425-455.

[32] Q. Pan, L. Zhang and G. Z. Dai, Two de-noising methods by wavelet transform, *IEEE Transactions on Signal Processing*, 47 (12) (1999) 3401-3406.

[33] L. Zhang, Q. Pan, H. C. Zhang and G. Z. Dai, On the determination of threshold in threshold-based de-noising by wavelet transform, *Acta Electronica Sinica*, 29 (3) (2001) 400-402.

[34] J. Serra, *Image analysis and mathematical morphology,* Academic Press, New York, USA (1982).

[35] S. Lou, X. Q. Jiang and P. J. Scott, Correlating motif analysis and morphological filters for surface texture analysis,

Measurement, 46 (2) (2013) 993-1001.
[36] F. Meyer, Iterative image transformations for an automatic screening of cervical smears, *Journal of Histochemistry and Cytochemistry*, 27 (1) (1979) 128-135.
[37] L. J. Zhang and D. B. Yang, Approach to extracting gear fault feature based on mathematical morphological filtering, *Chinese Journal of Mechanical Engineering*, 43 (2) (2007) 71-75.
[38] L. J. Zhang et al., Multiscale morphology analysis and its application to fault diagnosis, *Mechanical Systems and Signal Processing*, 22 (3) (2008) 597-610.
[39] S. J. Dong, B. P. Tang and Y. Zhang, A repeated single-channel mechanical signal blind separation method based on morphological filtering and singular value decomposition, *Measurement*, 45 (8) (2012) 2052-2063.
[40] Y. B. Dong et al., Faults diagnosis of rolling element bearings based on modified morphological method, *Mechanical Systems and Signal Processing*, 25 (4) (2011) 1276-1286.
[41] W. He, Z. N. Jiang and Q. Qin, A joint adaptive wavelet filter and morphological signal processing method for weak mechanical impulse extraction, *Journal of Mechanical Science and Technology*, 24 (8) (2010) 1709-1716.
[42] C. S. Li, Non-linear diagnosis method of rolling bearing fault, *Bearing*, 5 (2005) 35-37.

Ling-Jie Meng received the B.S. degree in Mechanical Engineering from Guilin University of Electronic Technology, China, in 2010. He is currently a postgraduate student in Wenzhou University. His research interests include faults detection of mechanical systems.

Jia-Wei Xiang received the B.S. degree in mechatronics from Hunan University, China, in 1997, the M.S. degree from Guangxi University, China, in 2003, and the Ph.D. from Xi'an Jiaotong University, China, in 2006. He is currently a professor at the college of Mechanical and Electrical Engineering, Wenzhou University, China. His research interests are the health monitoring of mechanical systems using numerical simulation and signal processing techniques.

Yong-Teng Zhong received the B.S. degree in Mechanical Engineering from Wuhan Textile University, China, in 2006, the M.S. degree from Guilin University of Electronic Technology, China, in 2010, and the Ph.D. from Nanjing University of Aeronautics and Astronautics, China, in 2014. He is currently a Lecturer at the college of Mechanical and Electrical Engineering, Wenzhou University, China. His research interests are the structural health monitoring of mechanical systems.

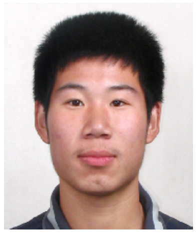

Wen-Lei Song received the B.S. degree in Mechanical Engineering from Laocheng University, China, in 2014. He is currently a postgraduate student in Wenzhou University. His research interests include faults detection of mechanical systems.